Strathprints Institutional Repository

Organic & Biomolecular Chemistry

PAPER

View Article Online
View Journal | View Issue

Cite this: *Org. Biomol. Chem.*, 2014, **12**, 1779

Lead identification and structure–activity relationships of heteroarylpyrazole arylsulfonamides as allosteric CC-chemokine receptor 4 (CCR4) antagonists†

Afjal H. Miah,[a] Royston C. B. Copley,[b] Daniel O'Flynn,[a] Jonathan M. Percy[c] and Panayiotis A. Procopiou*[a]

Received 6th December 2013,
Accepted 3rd February 2014

DOI: 10.1039/c3ob42443j

www.rsc.org/obc

A knowledge-based library of aryl 2,3-dichlorophenylsulfonamides was synthesised and screened as human CCR4 antagonists, in order to identify a suitable hit for the start of a lead-optimisation programme. X-ray diffraction studies were used to identify the pyrazole ring as a moiety that could bring about intramolecular hydrogen bonding with the sulfonamide NH and provide a clip or orthogonal conformation that was believed to be the preferred active conformation. Replacement of the core phenyl ring with a pyridine, and replacement of the 2,3-dichlorobenzenesulfonamide with 5-chlorothiophenesulfonamide provided compound **33** which has excellent physicochemical properties and represents a good starting point for a lead optimisation programme. Electronic structure calculations indicated that the preference for the clip or orthogonal conformation found in the small molecule crystal structures of **7** and **14** was in agreement with the order of potency in the biological assay.

Introduction

Chemokines are a group of small basic proteins, which together with their receptors mainly regulate the trafficking of leucocytes down a chemoattractant gradient.[1,2] Ten CC chemokine receptors have been identified so far and named as CCR1–CCR10. CCR4 belongs to the 7-TM domain G-protein-coupled receptor family and is mainly expressed in T helper 2 (Th2) cells. Th2 cytokines in inflamed tissues lead to eosinophilia, high levels of serum IgE and mast cell activation, all of which contribute to the pathogenesis of allergic diseases.[3] Thymus activation-regulated chemokine (TARC) and macrophage-derived chemokine (MDC), bind to the orthosteric binding site of CCR4.[4] Upon exposure to allergen, dendritic cells within tissue secrete MDC and TARC (also produced by endothelial cells) which can recruit Th2 cells from the circulation. The T cells can then migrate along this chemokine gradient to the dendritic cells. Upon maturation, the dendritic cells migrate from the inflamed tissue to local lymph nodes where the MDC and TARC which they produce may recruit further T cells to the inflammatory response. Elevated levels of TARC and MDC as well as accumulation of CCR4-positive cells have been observed in lung biopsy samples from patients with atopic asthma following allergen challenge.[5,6] Thus CCR4 antagonists represent a novel therapeutic intervention in diseases where CCR4 has a central role in pathogenesis, such as asthma, atopic dermatitis,[7] allergic bronchopulmonary aspergillosis,[8] cancer,[9] the mosquito-borne tropical diseases, such as Dengue fever,[10] and allergic rhinitis.[11] Progress in the discovery of small-molecule CCR4 antagonists as immunomodulatory agents was reviewed by Purandare and Somerville in 2006.[12] Since then a number of additional CCR4 antagonists have been published.[13–22] Among these antagonists are two pyrazine arylsulfonamides, the AstraZeneca 2,3-dichlorobenzenesulfonamide **1**[23] and Ono's 4-methylbenzenesulfonamide **2** (Fig. 1).[24] Recently we have reported a class of indazole arylsulfonamides including **3**, which we believe is the first small-molecule clinical candidate targeting the CCR4 receptor.[25,26] Furthermore, the pyrazine and indazole arylsulfonamide CCR4 antagonists **1–3** bind at an intracellular allosteric binding site, which is different from the extracellular binding site where lipophilic amine antagonists such as **4** to **6** bind.[27] The two allosteric

[a]*Allergy & Inflammation DPU, Respiratory TAU, GlaxoSmithKline Medicines Research Centre, Gunnels Wood Road, Stevenage, Hertfordshire SG1 2NY, UK. E-mail: pan.a.procopiou@gsk.com; Fax: +44 (0)1438 768302; Tel: +44 (0)1438 762883*

[b]*UK Analytical Chemistry, Platform Technology & Science, GlaxoSmithKline Medicines Research Centre, Gunnels Wood Road, Stevenage, Hertfordshire SG1 2NY, UK*

[c]*WestCHEM Department of Pure and Applied Chemistry, University of Strathclyde, 295 Cathedral Street, Glasgow, G1 1XL, UK*

†Electronic supplementary information (ESI) available. CCDC 975458–975461. For ESI and crystallographic data in CIF or other electronic format see DOI: 10.1039/c3ob42443j

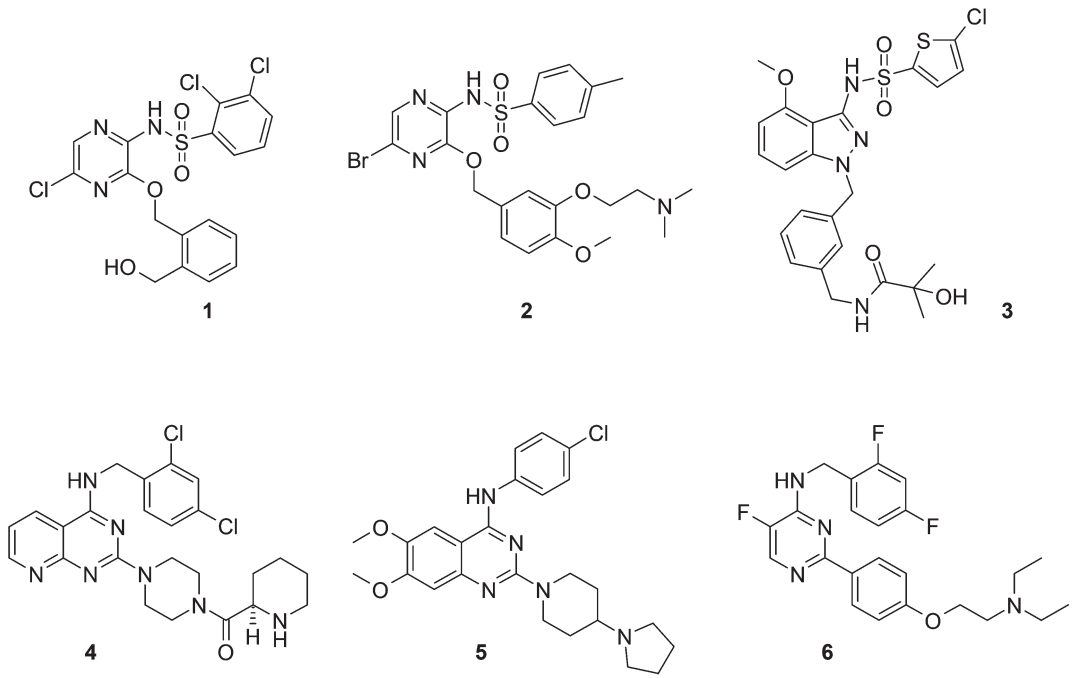

Fig. 1 Structures for some recently published CCR4 antagonists.

binding sites are distinct from each other and from the orthosteric site where TARC and MDC bind.

Indazole **3** was progressed to human pharmacokinetic and pharmacodynamic studies and the results were reported very recently.[28] The compound was generally safe and well tolerated by healthy male subjects. Following intravenous dosing, **3** displayed rapid, biphasic distribution and slow elimination ($t_{1/2}$ = 13.5 h). Following oral dosing, blood levels reached C_{max} rapidly (1.0–1.5 h), but bioavailability was low (16%). At a dose of 1.5 g **3** inhibited TARC-induced actin polymerisation reaching a mean CCR4 occupancy of 74%. Based on the low oral bioavailability of **3** its further progression was halted. Herein we present our attempts to identify an alternative lead series of sulfonamide CCR4 antagonists, suitable for an optimisation programme to develop a potential back-up compound to indazole **3**. We sought a low molecular weight and higher potency compound that would bind to the intracellular sulfonamide binding site. In our recent publication we reported a low energy conformation based on small molecule X-ray diffraction studies, where the plane normals of the indazole core and the sulfonamide ring were positioned at right angles, with an intramolecular hydrogen bond between the sulfonamide NH and the OMe group.[26] Furthermore a range of groups including –F, –Cl, –OH, –CN, $–CHF_2$, –COMe, $–CH_2OH$, –CH(OH)Me and $–CMe_2OH$ were investigated as alternative hydrogen bond acceptors, and it was found that the four hydroxyl containing compounds had increased potency in the human CCR4 GTPγS assay. However, this increase did not translate in the human whole blood assay, or to their pharmacokinetic properties. The group which conferred optimal properties was found to be the methoxy group, which was retained in the subsequent lead optimisation that provided **3** as the clinical candidate. Intramolecular hydrogen bonding has been used as a means to reduce Sildenafil's polar group interaction (pyrimidine NH) with water and hence increase its oral absorption.[29] Further uses of intramolecular hydrogen bonding to increase membrane permeability, water solubility, and lipophilicity were recently reported by Kuhn for a variety of motifs based on X-ray crystal structure analysis.[30]

Results and discussion

Antagonist potency was determined by a [^{35}S]-GTPγS radioligand competition functional assay using recombinant CCR4-expressing CHO cell membranes adhered to WGA-coated Leadseeker SPA beads in pH 7.4 buffer.[31] A secondary assay using human whole blood was used as a screen to determine potency against the native receptor for the more potent compounds in the primary assay. The assay quantified cytoskeletal reorganisation (formation of filamentous (F-) actin) which occurs in a variety of cells in response to chemoattractants and is a prelude to chemotaxis. Calculated partition coefficient (*clog P*), chromatographic log *D* (chrom log *D* at pH 7.4) and ChemiLuminescent Nitrogen Detection (CLND) kinetic solubility are included for all test compounds in this study. The high throughput CLND solubility assay involved addition of aqueous buffer to a test compound DMSO solution over a period of time until the compound precipitated. Ligand efficiency (LE) was obtained from the equation LE = $-1.36 \times pIC_{50}$/HAC, where HAC is the heavy atom count (number of non-hydrogen atoms present in the molecule), with a desirable figure of LE being >0.3.

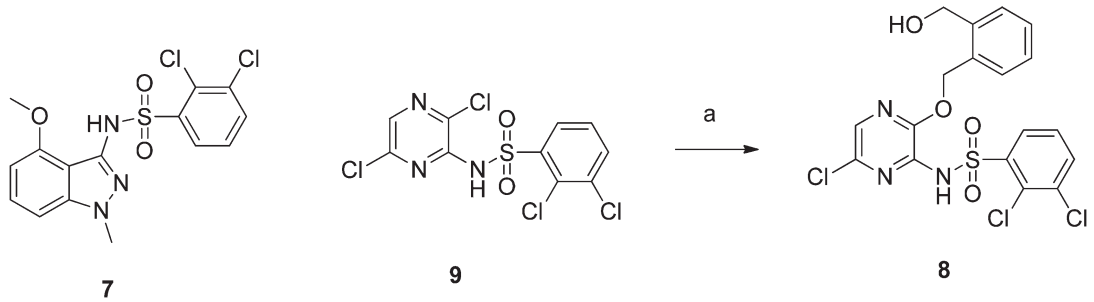

Scheme 1 Reagents and conditions: (a) 1,2-phenylenedimethanol (5 equiv.), *tert*-BuOK (7.5 equiv.), THF, NMP, 5 h, 17%.

Sulfonamide **7**, the starting point for the indazole lead optimisation process, was used as a reference compound for the analogues made in this investigation. Compounds of interest had to have higher potency than **7** in the GTPγS assay ($pIC_{50} > 6.2$), and better physicochemical properties (*c*log $P <$ 3.48; chrom log $D < 5.3$; CLND solubility > 116 μg mL^{-1}). The novel pyrazine **8**, a regioisomer of the AstraZeneca CCR4 antagonist **1**, was used as a standard in the GTPγS assay. Compound **8** was prepared from **9** and 1,2-phenylenedimethanol by regioselective displacement of the 3-chloro substituent (Scheme 1), and its structure was unambiguously confirmed by an X-ray diffraction study (Fig. 2). In both independent molecules present in the crystal structure, the sulfonamide hydrogen atom was located and refined approximately in the plane of the pyrazine ring, allowing a favourable electrostatic interaction to the ether oxygen in the same molecule. The influence on the conformation of these intramolecular interactions involving five-membered rings is uncertain given the classical intermolecular hydrogen bonds from the sulfonamide hydrogen atoms that are also present in the crystal structure (see ESI† for details).

The indazole sulfonamide **7** was also crystallised and suitable crystals were obtained for an X-ray diffraction study. The structure contained two crystallographically independent molecules, both of which possessed an intramolecular hydrogen bond between the sulfonamide NH and the methoxy ether oxygen atom, as we reported previously in the case of the 5-chlorothiophenesulfonamide analogue of **7**.[26] The conformations of the two independent molecules are related by a pseudo-inversion centre. The metric details of the intramolecular hydrogen bonds are as follows: for the first molecule (shown in Fig. 3), N–H 0.80(2) Å, H···O 2.49(2) Å; N···O 3.011(2) Å; and ∠N–H···O 124(2)°; and for the second molecule, N–H 0.79(2) Å, H···O 2.47(2) Å; N···O 3.0238(19) Å; and ∠N–H···O 129(2)°. A consequence of the hydrogen bonds is to allow the plane normals to the 2,3-dichlorobenzene rings and the indazole rings to be approximately orthogonal [81.15(5)° and

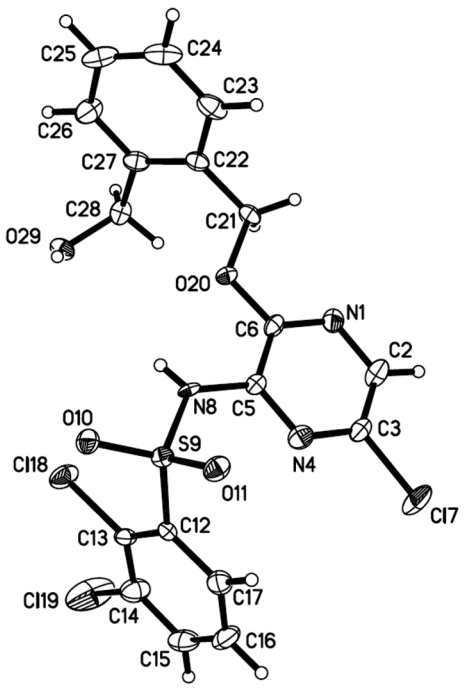

Fig. 2 A view of one of the independent molecules from the X-ray crystal structure of **8**. Anisotropic atomic displacement ellipsoids for the non-hydrogen atoms are shown at the 50% probability level. Hydrogen atoms are displayed with an arbitrarily small radius.

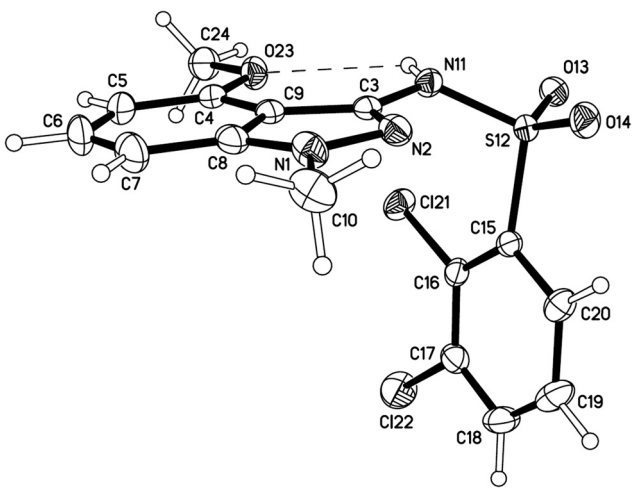

Fig. 3 A view of one of the independent molecules from the X-ray crystal structure of **7**. Anisotropic atomic displacement ellipsoids for the non-hydrogen atoms are shown at the 50% probability level. Hydrogen atoms are displayed with an arbitrarily small radius. The intramolecular hydrogen bond is indicated by a dashed line.

75.92(5)° for the above two molecules respectively]. This conformation was not previously reported for [5,6] bicyclic cores containing any combination of carbon, nitrogen and oxygen atoms, and being substituted with a sulfonamide moiety and an oxygen atom prior to our previous disclosure.[26] It is postulated that this conformation might be a preferred one for increased binding activity.

Investigations to identify other hit series began with the introduction of an *ortho* substituent into the simplest 2,3-dichlorobenzenesulfonamide **10** (pIC_{50} = 5.3) (Scheme 2 and Table 2). Three groups were introduced, MeO–, MeCO–, MeCH(OH)– and the respective analogues **11–13** were screened in the GTPγS assay, which confirmed that the MeO– group increased the potency of **10** by ten-fold (Table 1). Prototypes **7** and **11** were equipotent (pIC_{50} 6.2), with **11** being more lipophilic (*c*log *P* 3.93 *vs.* 3.48 and chrom log *D* 6.1 *vs.* 5.3), and with a correspondingly lower CLND solubility (20 μg *vs.* 116 μg mL^{-1}). The ketone **12** and alcohol **13** were less potent than the methoxy analogue **11** confirming our earlier findings.

In our search for alternative groups to the MeO– group we envisaged that a 5-membered heteroaryl ring containing two or more heteroatoms, and placed *ortho* to the sulfonamide group might be a good hydrogen bond acceptor for the sulfonamide NH, thus driving the 2,3-dichlorophenyl and phenyl ring to which the sulfonamide group is attached, to be orthogonal as in the case of **7**. Five compounds possessing 5-membered rings, including pyrazole, triazole, tetrazole, oxazole and oxadiazole were synthesised from commercially available substituted anilines and 2,3-dichlorobenzenesulfonyl chloride to give analogues **14–18**. These analogues were screened *in vitro* and the data are presented in Table 1. Pyrazole **14** was the most potent of the six heterocyclic analogues, with a pIC_{50} of 6.6 and LE of 0.39. In addition it was weakly active in the human whole blood assay (pA_2 5.3), whereas the other heterocyclic analogues were not active. Its lipophilicity however was unacceptably high (*c*log *P* 4.08 and chrom log *D* 6.4) as was its low solubility (48 μg mL^{-1}). A small molecule X-ray crystal structure of the phenyl pyrazole **14** was obtained (Fig. 4) which confirmed the existence of an intramolecular hydrogen bond between the sulfonamide NH and a nitrogen in the pyrazole

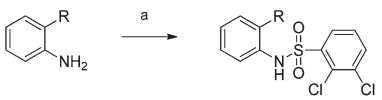

Scheme 2 Reagents and conditions: (a) 2,3-dichlorobenzenesulfonyl chloride, pyridine.

Table 1 *In vitro* data pIC_{50} for human CCR4 GTPγS binding assay, calculated log *P*, ligand efficiency, measured chrom log *D* at pH 7.4 and CLND solubility

Cmpd	GTPγS pIC_{50} ± SEM (*n*)	*c*log *P*	LE	Chrom log *D*	CLND solub. (μg mL^{-1})
7	6.22 ± 0.03 (2)	3.48	0.35	5.3	116
8	8.2 ± 0.0 (252)	3.97	0.38	4.0	153
10	5.3 ± 0.2 (2)	3.99	0.40	5.8	3
11	6.2 ± 0.0 (2)	3.93	0.42	6.1	20
12	<4.5 (2)	3.95	0.29	6.45	5
13	5.24 ± 0.03 (3)	2.70	0.34	5.0	132
14	6.63 ± 0.08 (6)	4.08	0.39	6.4	48
15	5.8 ± 0.2 (4)	3.0	0.34	3.3	180
16	5.9 ± 0.5 (4)	3.23	0.35	2.9	233
17	5.1 ± 0.1 (2)	3.79	0.30	4.4	123
18	<4.5 (2)	2.84	0.25	6.3	8
19	5.8 ± 0.1 (2)	3.26	0.34	6.7	34
20	5.46 ± 0.07 (2)	3.26	0.33	2.85	164
23	7.2 ± 0.1 (4)	3.26	0.43	3.72	203
26	6.6 ± 0.4 (2)	3.26	0.39	3.23	76
30	6.83 ± 0.01 (2)	2.48	0.40	3.0	181
33	7.2 ± 0.2 (2)	2.66	0.47	2.84	133

Table 2 Structure of substituent R in Scheme 2

Compound number	R	Compound number	R
10	–H	**15**	
11	–OMe	**16**	
12		**17**	
13	 (a)	**18**	
14			

(a) Compound **13** was obtained by reduction of **12** with sodium borohydride in methanol.

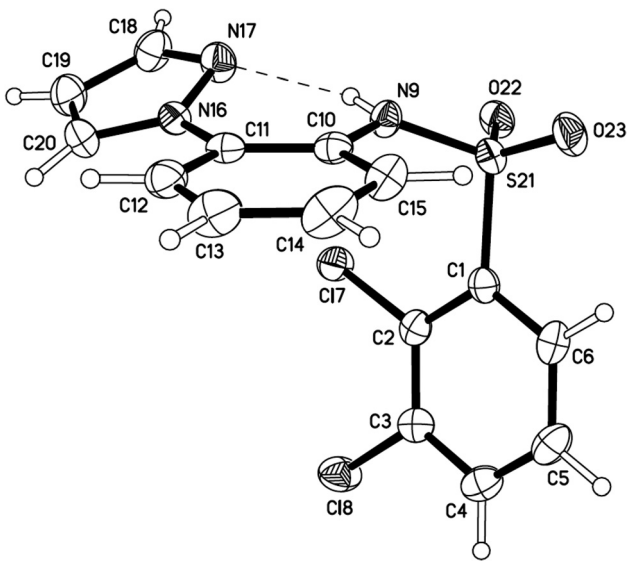

Fig. 4 X-ray crystal structure of phenyl pyrazole **14**. Anisotropic atomic displacement ellipsoids for the non-hydrogen atoms are shown at the 50% probability level. Hydrogen atoms are displayed with an arbitrarily small radius. The intramolecular hydrogen bond is indicated by a dashed line.

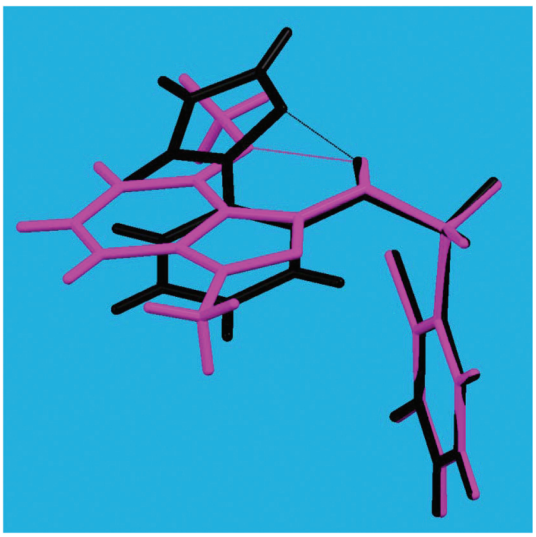

Fig. 5 Least-squares fit (RMS = 0.05 Å) of the 12 non-hydrogen atoms in the sulfonamide side-chain of indazole **7** (magenta) and pyrazole **14** (black). The intramolecular hydrogen bonds are depicted as dotted lines.

ring [N–H 0.81(2) Å, H···N 1.95(2) Å; N···N 2.638(3) Å; and ∠N–H···N 143(2)°]. Plane normals to the two phenyl rings were inclined at 76.65(7)°.

The structures of **7** (the independent molecule shown in Fig. 3) and **14** were overlaid and are shown in Fig. 5. The overlay was done on the basis of a least-squares fit for the non-hydrogen atoms in the sulfonamide side-chains. The RMS for this fit was just 0.05 Å, indicating how close the conformations are for this moiety. The remainder of the molecules, although clearly different, occupy a similar region of space relative to the atoms fitted, potentially driven by the presence of the intramolecular bonds.

An X-ray crystal structure of the phenyl tetrazole **16**, was obtained (Fig. 6), which showed that the sulfonamide NH did not take part in an intramolecular hydrogen bond but instead was associated with an intermolecular hydrogen bond to N17 [N–H 0.80(2) Å, H···N 2.34(2) Å; N···N 3.107(2) Å; and ∠N–H···N 161(2)°]. With this arrangement, the rings at either end of the sulfonamide group are somewhat less orthogonal, having their normals inclined at 65.65(7)°.

Fig. 7 shows an overlay of the non-hydrogen atoms of the 2,3-dichlorobenzenesulfonamide moiety in **14** and **16**, indicating that as before, the conformations of these groups are nearly identical. The RMS is again just 0.05 Å. However, relative to the fitted atoms, the conformations of the rest of the **14** and **16** molecules are clearly different. In **14**, the S21–N9–C10–C11 torsion angle (that defines the orientation of the central phenyl ring relative to the sulfonamide group) is −150.44(18)°, whereas for **16**, without the intramolecular hydrogen bond, the equivalent torsion angle is 78.8(2)°. This represents a relative rotation of the phenyl ring of approximately 131°.

Clearly, in the solid state, the various intermolecular packing forces play a large role in the conformations adopted

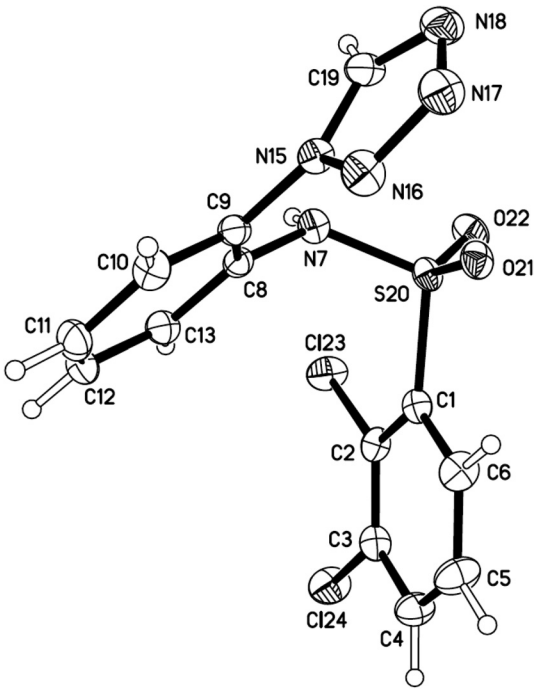

Fig. 6 X-ray crystal structure of phenyl tetrazole **16** showing the absence of an intramolecular hydrogen bond between the NH of the sulfonamide and the tetrazole ring. Anisotropic atomic displacement ellipsoids for the non-hydrogen atoms are shown at the 50% probability level. Hydrogen atoms are displayed with an arbitrarily small radius.

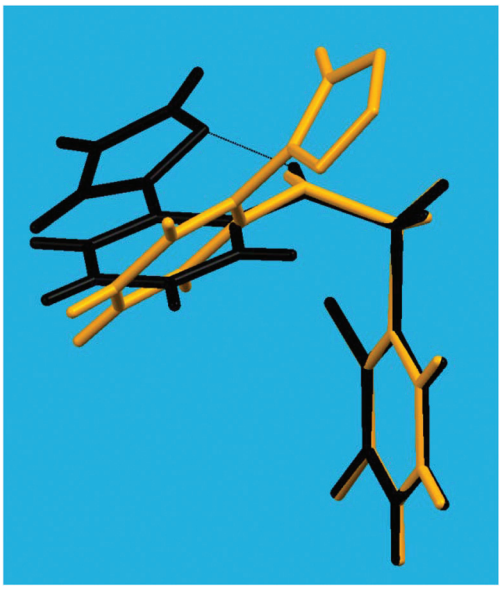

Fig. 7 Least-squares fit (RMS = 0.05 Å) of the 12 non-hydrogen atoms in the sulfonamide side-chain of pyrazole **14** (black) and phenyl tetrazole **16** (orange). The intramolecular hydrogen bond in the former is depicted as a dotted line.

and we do not wish to suggest that the presence of the intramolecular interaction is the primary or only driver. Nonetheless, having shown that the pyrazole **14** can adopt a

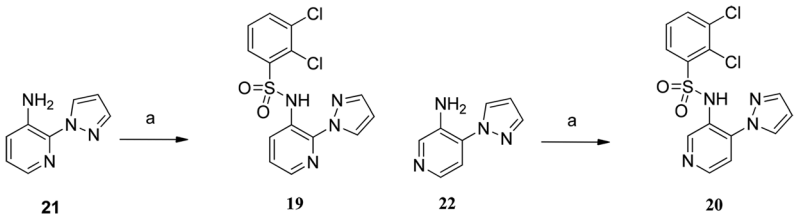

Scheme 3 Reagents and conditions: (a) 2,3-dichlorobenzenesulfonyl chloride, pyridine, 20 °C, 18 h.

conformation in the solid state similar to those of the indazole sulfonamides and pyrazine **8**, it was decided to focus on further analogues of **14**, optimising the physicochemical properties (*c*log *P*, chrom log *D* and solubility). In addition, the core ring of **14** is a substituted aniline, which is not very attractive in a drug candidate, because of potential genotoxicity issues.[32] One way of bypassing such a problem is to introduce a nitrogen atom into the phenyl core, which will also lower the lipophilicity, and increase its solubility. The synthesis of analogues containing a nitrogen atom at each one of the four available positions on the core ring of **14** was undertaken. The two pyridyl analogues **19** and **20** were prepared from the corresponding commercially available amines **21** and **22** in 60% and 47% yield respectively (Scheme 3).

The synthesis of pyrazolyl-5-pyridine sulfonamide **23** is outlined in Scheme 4. 3-Bromopyridin-2-amine (**24**) was reacted with pyrazole, in the presence of copper iodide, potassium carbonate and *N*,*N*′-dimethylethylenediamine in xylene at 142 °C to afford 3-(1*H*-pyrazol-1-yl)pyridin-2-amine **25** in 50% yield.[33] Reaction with 2,3-dichlorobenzenesulfonyl chloride in pyridine afforded the desired sulfonamide **23** in 41% yield.

The synthesis of the pyrazolyl-3-pyridine sulfonamide **26** is shown in Scheme 5 and involved reaction of 3-fluoro-4-nitropyridine **27** with pyrazole in the presence of sodium hydride in NMP at 100 °C to give **28** in 64% yield. Reduction of the nitro group of **28** with tin(II) chloride gave **29** in 68% yield. Reaction of the latter with 2,3-dichlorobenzenesulfonyl chloride in pyridine afforded the desired sulfonamide **26** in 51%.

Replacement of the phenyl core of **14** with a pyrazine ring would provide an even more hydrophilic analogue than the corresponding pyridines. The synthesis of analogue **30** is shown in Scheme 6 and it commenced with reaction of 3-bromo-pyrazine-2-amine **31** with 2,3-dichlorobenzenesulfonyl chloride to give sulfonamide **32**, followed by displacement of bromine by pyrazole in the presence of sodium hydride in NMP to give **30** in 71% yield.

The four pyridine analogues **19**, **20**, **23**, **26** and pyrazine **30** were tested *in vitro* and the data is shown in Table 1. Pyridines **19** and **20** had disappointingly weak affinities for the CCR4 receptor, whereas **26** was equipotent to **14**. Pyridine **23** however, was significantly more potent (pIC_{50} 7.2), its *c*log *P* was low at 3.26, and its chrom log *D* was 3.72. Furthermore, its ligand efficiency was 0.43 making it one of the most attractive compounds in this study. In addition its CLND solubility increased to 203 μg mL^{-1}. In contrast the pyrazine **30**, despite its even lower *c*log *P* and chrom log *D*, had a slightly lower affinity (pIC_{50} 6.8) and a correspondingly lower LE (0.40). The reason for **23** being the most potent regioisomer of the four pyridine analogues was not investigated any further. An explanation for the higher potency of **23**, might be a favourable interaction between the pyridine nitrogen when it is situated *ortho* to the sulfonamide group and the receptor, and this is also true in the pyrazine **30**, which was the second most potent analogue in the series.

In a final iteration to improve the potency and ligand efficiency of **23**, we examined the replacement of the 2,3-dichlorobenzenesulfonamide group. In our investigation of the indazole sulfonamide series the 5-chlorothiophenesulfonamide group was identified as a superior group as it had a

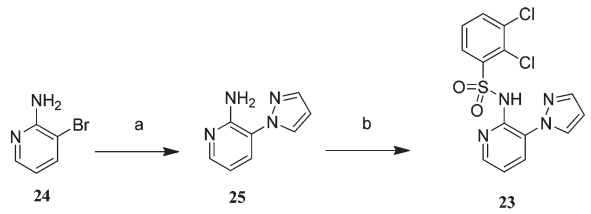

Scheme 4 Reagents and conditions: (a) Pyrazole, K_2CO_3, CuI, *N*,*N*-dimethylethylenediamine, *p*-xylene, 142 °C, 72 h, 50%; (b) 2,3-dichlorobenzenesulfonyl chloride, pyridine, 20 °C, 3 h, 41%.

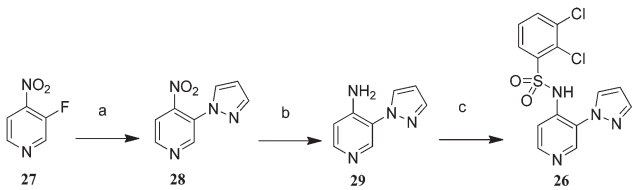

Scheme 5 Reagents and conditions: (a) NaH, pyrazole, NMP, 0–100 °C, 18 h, 64%; (b) $SnCl_2$, conc. HCl, MeOH, 20 °C, 48 h, 68%; (c) 2,3-dichlorobenzenesulfonyl chloride, pyridine, 20 °C, 8 h, 51%.

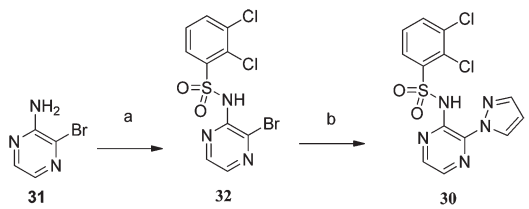

Scheme 6 Reagents and conditions: (a) NaH, DME, 0 °C, 30 min, 2,3-dichlorobenzenesulfonyl chloride, 20 °C, 8 h, 73%; (b) NaH, pyrazole, NMP, 0 °C, 5 min, 100 °C, 18 h, 71%.

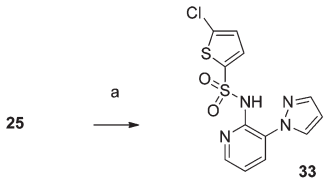

Scheme 7 Reagents and conditions: (a) 5-chlorothiophene-2-sulfonyl chloride, pyridine, 20 °C, 3 h, 57%.

lower molecular weight and was also less lipophilic than the 2,3-dichlorobenzenesulfonamide.

The sulfonamide **33** was prepared from **25** and 5-chlorothiophene-2-sulfonyl chloride in pyridine in 57% yield (Scheme 7). The lipophilicity of **33** (*c*log *P* 2.66) was the lowest in this study, as was its chrom log *D* (2.84). It was equipotent to **23** (pIC_{50} 7.2) and its LE increased to 0.47 making it the most ligand-efficient compound of this study. In addition its molecular weight was low (341), the number of hydrogen bond acceptors (6) and number of hydrogen bond donors (1) are well within the Lipinski guidelines. Its polar surface area was 76, well below the recommended limit of 140 Å^2. Furthermore, **33** was tested in the human whole blood assay and it was weakly active (pA_2 5.2). These encouraging data make **33** a good starting point for a lead-optimisation study.

Conformational analysis

Conformations identified from crystal structures may not be representative of states occupied in solution due to the presence of packing forces, so electronic structure calculations were used to explore this more fully. Structures corresponding to **7**, **14** and **16** were built in Spartan'08[34] and Monte Carlo conformational searching was carried out using the PM3 semi-empirical method. Relatively small sets of conformers (10 typically) were obtained and geometry optimisation calculations were carried out for all members of the sets using the B3LYP functional[35,36] and the 6-31G* and 6-31+G* basis sets, *in vacuo* and in water (Truhlar's SM8 model[37,38] was applied). Single point energy calculations were also carried out (*in vacuo*) with the larger 6-311+G** basis set (using the dual basis set approximation implemented in Spartan'08). There were no significant basis set effects on the rankings of conformer energies or on the geometries obtained.

Full frequency calculations were carried out with the smaller 6-31G* basis (*in vacuo* and in water) to identify minima unequivocally and show that electronic energies provide a reliable guide to free energies (see the ESI† for more details). An excellent correlation (R^2 = 0.991) was obtained between relative electronic energies, E_{rel} and relative free energies G_{rel} for all the conformers of **7** and **14** (B3LYP/6-31G*, *in vacuo* and in water). Electronic energies obtained with the larger basis set (B3LYP/6-31+G* *in vacuo* and in water) are therefore used as the basis for the subsequent discussion, avoiding the much higher cost of the full frequency calculations.

The application of the solvation model affects both energies and geometries; the calculated dipoles were bigger for the structures in water, consistent with the much higher polarity of the medium. All the energies and geometries referred to subsequently were calculated in water.

Clip-shaped or orthogonal conformations (corresponding to those revealed in the crystal structures of **7**, **14** and to a lesser extent, **16**) were identified, though closely-related and energetically-similar conformations were also found. The clip is formed from the dichlorophenyl ring and the arene which bears the hydrogen bond acceptor/donor array; the angles between the planes measured from the optimised structures are 77° for **7**, 66° for **14** and 62° for **16** (Fig. 8).

The clip-shaped or orthogonal conformations are shown in the left-hand column of Fig. 9. For pyrazolyl species **14**, the lowest energy species corresponds to the clip conformation; the next lowest conformer is also a clip or orthogonal at +1.2 kcal mol^{-1}. The dichlorophenyl ring has flipped through 180° *via* a rotation in the sulfonamido group. The next conformation at +2.1 kcal mol^{-1} is more extended. The same behaviour was observed for indazole **7**, with a pair of clip-shaped conformers 1.4 kcal mol^{-1} apart; however, in this case a more extended conformation is much more competitive at +0.2 kcal mol^{-1}.

Tetrazole **16** behaved differently; the lowest energy conformation is clip-shaped but the dichlorophenyl ring is flipped over into a different orientation, presenting the chlorine atoms away from the hydrogen bond acceptor/donor array. The clip-shaped conformation corresponding to the minima for **7** and **14** lies 0.7 kcal mol^{-1} higher in energy.

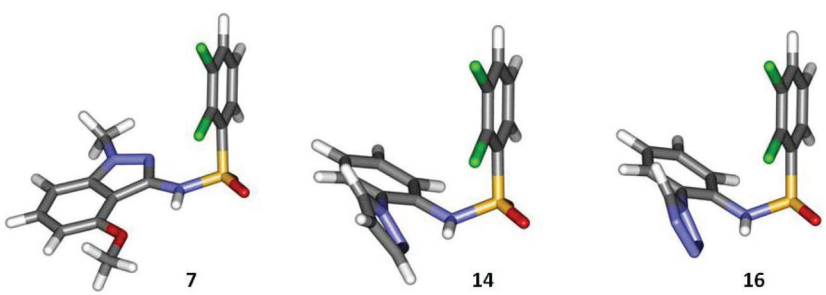

Fig. 8 Stick diagrams of orthogonal conformers calculated (B3LYP/6-31+G* in water [SM8]) for **7**, **14** and **16**.

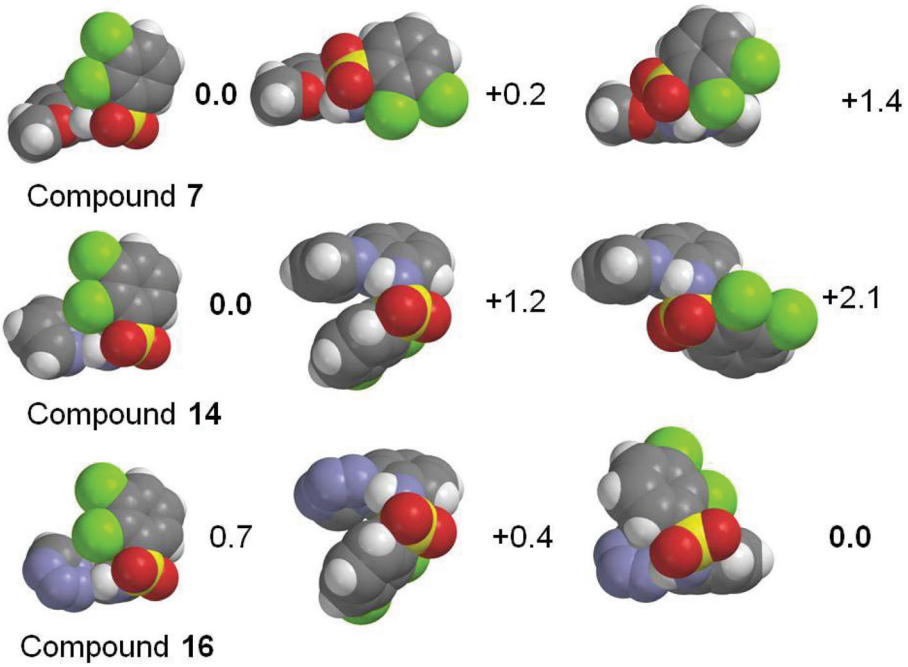

Fig. 9 CPK models of low energy conformers (E_{rel} in kcal mol^{-1}) optimised (B3LYP/6-31+G* in water [SM8]) for **7**, **14** and **16**. The clip or orthogonal conformers form the left-hand column.

The lowest energy conformation found for **16** still contains an intramolecular hydrogen bond, unlike the arrangement found in the crystal structure; with an isolated molecule, opening the intramolecular hydrogen bond (IHB) leaves the hydrogen bond acceptor and donor sites unsatisfied, which will have an enthalpic cost. However, the lowest energy conformation which lacks the IHB, lies only 1.7 kcal mol^{-1} above the global minimum, whereas opening the IHB in **14** appears to cost 7.5 kcal mol^{-1}. Though the geometries of **14** and **16** should be broadly similar, there are significant differences between the two azoles. Pyrazole is significantly more basic (*ca.* 5 pK_a units) than tetrazole, and the IHB acceptor site in **16** is not the usual site of tetrazole protonation (see the ESI† for more details). The apparent difference in IHB strength therefore appears reasonable. Searching also revealed the conformation found in the crystal for **16**, at 5.1 kcal mol^{-1} above the global minimum.

These energy differences are small, but even very modest differences in binding energies can affect potency significantly; the order of preference for the clip or orthogonal conformation found in the small molecule crystal structures of **7** and **14** is the same (**14** > **7** > **16**) as the order of potency in the GTPγS assay data.

Conclusion

The aim of this study was to identify a lead compound suitable for the start of a lead-optimisation programme to deliver a CCR4 antagonist as a potential back-up to the clinical candidate **3**. The study began by examining a number of *ortho*-substituents capable of hydrogen bonding to a sulfonamide NH. It was envisaged that a five-membered heterocyclic ring with two or more heteroatoms would be capable of hydrogen bonding to bring about an orthogonal or clip conformation, which then binds to the receptor preferentially. X-ray crystal structure determinations helped to identify the pyrazole ring as a moiety that could bring about the desired hydrogen bonding and conformation. Replacement of the core phenyl ring with a pyridine and replacement of the 2,3-dichlorobenzenesulfonamide with 5-chlorothiophenesulfonamide provided compound **33** with excellent physicochemical properties, and suitable for further elaboration. Conformational analysis performed on compounds **7**, **14** and **16** was in agreement with the order of preference for the clip or orthogonal conformation found in the small molecule crystal structures, and the order of potency in the GTPγS assay.

Experimental

Organic solutions were dried over anhydrous Na_2SO_4, $MgSO_4$ or using a hydrophobic frit. TLC was performed on Merck 0.25 mm Kieselgel 60 F_{254} plates. Products were visualised under UV light and/or by staining with aqueous $KMnO_4$ solution. LCMS analysis was conducted on an Acquity UPLC BEH C_{18} column (50 mm × 2.1 mm ID, 1.7 μm packing diameter) eluting with 0.1% formic acid in water (solvent A), and 0.1% formic acid in MeCN (solvent B), using the following elution gradient 0.0–1.5 min 3–100% B, 1.5–1.9 min 100% B, 1.9–2.0 min 100–3% B, at a flow rate of 1 mL min^{-1} at 40 °C. The UV detection was an averaged signal from wavelength of

210 nm to 350 nm, and mass spectra were recorded on a mass spectrometer using alternate-scan electrospray positive and negative mode ionization (ESI+ve and ESI−ve). Column chromatography was performed on a Flashmaster II system. Purifications by mass-directed auto-preparative HPLC (MDAP) was conducted on a Sunfire C18 column (150 mm × 30 mm i.d. 5 μm packing diameter) at ambient temperature eluting with 0.1% formic acid in water (solvent A) and 0.1% formic acid in MeCN (solvent B), using an appropriate elution gradient over 15 or 25 min at a flow rate of 40 mL min^{-1} and detecting at 210–350 nm at room temperature. Mass spectra were recorded on Micromass ZMD mass spectrometer using electrospray positive and negative mode, alternate scans. The software used was MassLynx 3.5 with OpenLynx and FractionLynx options.

^{1}H NMR spectra were recorded at 400, 500 or 600 MHz. Chemical shifts (δ) are expressed in ppm relative to tetramethylsilane. ^{13}C NMR spectra were recorded at 101, 126 or 150 MHz. ^{1}H and ^{13}C NMR spectra were recorded using the deuterated solvent as the lock and the residual solvent as the internal reference. In the cases indicated solid $NaHCO_3$ was added to the NMR solution to sharpen up the line-widths of the ^{13}C signals, as some signals were so broad that did not show up in the absence of base. It is assumed that the original samples had very broad signals due to inter-conversion between different forms at an intermediate rate over the NMR timescale. These different forms might be due to the zwitterionic nature of the compounds. Adding the base generated the sodium salt and created a single form with a sharp set of lines.

High resolution mass spectra were acquired on a Micromass Q-Tof 2 hybrid quadrupole time-of-flight mass spectrometer coupled to HPLC. LC analysis for HRMS was conducted on a Phenomenex Luna C18 (2) column (100 mm × 2.1 mm, 3 μm particle size), eluting with 0.1% formic acid water (solvent A), and 0.1% formic acid in MeCN (solvent B), using the following elution gradient 0–2 min 5% B, 2–8 min 5–100% B, 8–10.5 min 100% B, 10.5–11.5 min 100–5% B, 11.5–14 min 5% B, at a flow rate of 0.5 mL min^{-1}, at 35 °C. The elemental composition was calculated using MassLynx v4.1 for the $[M + H]^+$. The purity of all compounds screened in the biological assays was ≥95%, unless otherwise specified. Melting points were determined on a Stuart SMP40 automatic melting point apparatus. Starting materials were commercially available unless otherwise specified.

The four single crystal X-ray diffraction studies on **7**, **8**, **14** and **16** were carried out at 150 K using Mo-Kα X-radiation (λ = 0.71073 Å). Crystal data for each compound are given in the sections below. A description of the refinement and the full tables associated with each crystal structure are given in the ESI.† Crystallographic information files have been deposited with the Cambridge Crystallographic Data Centre (CCDC). CCDC 975458–975461 contain the supplementary crystallographic data for this paper.

2,3-Dichloro-*N*-[1-methyl-4-(methyloxy)-1*H*-indazol-3-yl]-benzenesulfonamide (7)

A solution of 4-methoxy-1*H*-indazol-3-amine[39] (2.38 g, 13.4 mmol) in pyridine (50 mL) was treated portionwise with 2,3-dichlorobenzenesulfonyl chloride (3.36 g, 13.7 mmol) at 20 °C, and the reaction mixture was stirred for 18 h. An additional portion of 2,3-dichlorobenzenesulfonyl chloride (1 g, 4 mmol) was added and the mixture was stirred at room temperature for 18 h. The reaction mixture was partitioned between dichloromethane (250 mL) and water (250 mL). The organic phase was washed with 2 M hydrochloric acid (100 mL), dried and evaporated under reduced pressure. The residue was purified by chromatography on a silica (100 g) cartridge eluting with a gradient of 0–100% ethyl acetate–cyclohexane over 60 min. The appropriate fractions were combined and evaporated *in vacuo* to give **7** (2.51 g, 48%) as an off-white solid: ^{1}H NMR (500 MHz, DMSO-d_6) δ = 10.43 (s, 1H), 7.91 (dd, J = 8.0, 1.0 Hz, 1H), 7.85 (dd, J = 8.0, 1.0 Hz, 1H), 7.47 (t, J = 8.0 Hz, 1H), 7.26 (t, J = 8.0 Hz, 1H), 7.08 (d, J = 8.0 Hz, 1H), 6.46 (d, J = 8.0 Hz, 1H), 3.86 (s, 3H), 3.64 (s, 3H); ^{13}C NMR (126 MHz, DMSO-d_6) δ = 153.5, 142.9, 141. 6, 134.8, 134.5, 134.3, 129.9, 129.6, 128.6, 128.5, 110.4, 102.8, 100.4, 55.5, 36.0; LCMS (ESI) RT = 1.05 min, 100% pure, m/z 386, 388 $[M + H]^+$. Anal. Calcd for $C_{15}H_{14}Cl_2N_3O_3S$ = 386.0128. Found = 386.0125 $[M + H]^+$. Crystal data: $C_{15}H_{13}Cl_2N_3O_3S$; M = 386.24; colourless wedge; spontaneous crystallisation from methanol, 10% 2 M HCl; 0.82 × 0.62 × 0.34 mm; triclinic; space group, $P\bar{1}$ (no. 2); unit cell dimensions, a = 7.9294(12) Å, b = 12.763(2) Å, c = 16.761(3) Å, α = 96.664(17)°, β = 99.981(17)°, γ = 97.378(14)°, V = 1640.1(5) Å^3; Z = 4; d_{calc} = 1.564 Mg m^{-3}; and μ(Mo-Kα, λ = 0.71073 Å) = 0.543 mm^{-1}.

2,3-Dichloro-*N*-(3,6-dichloropyrazin-2-yl)benzenesulfonamide (9)

A solution of 3,6-dichloropyrazin-2-amine[40] (6.1 g, 37 mmol) in DME (300 mL) was treated with solid NaH (60% oil dispersion, 7.5 g, 190 mmol) over 45 min at room temperature. After the addition was complete the mixture was warmed to 50 °C for 1 h. At this temperature, 2,3-dichlorobenzenesulfonyl chloride (11.9 g, 49 mmol) was added over 1 h and the mixture stirred for a further 30 min at 50 °C. The solution was cooled in an ice-bath and treated with 5% aqueous citric acid solution. The resulting mixture was partitioned between ethyl acetate and brine, the organic layer separated, dried (sodium sulfate) and concentrated to an orange solid (16 g). The residue was triturated with diethyl ether to give 11 g of the crude product, which was purified by chromatography in a gradient of ethyl acetate–petrol to MeOH–EtOAc (starting with 30% EtOAc in petrol), and re-purified by chromatography using a gradient of 0–30% MeOH–dichloromethane to give two fractions of varying purity. The first was triturated with diethyl ether to give pure **9** (3.2 g, 23%). The second fraction was further purified by chromatography using a gradient of 10% MeOH–dichloromethane to give pure **9** (2 g, 14%) and some impure fractions. The impure fractions were concentrated and triturated with diethyl ether to give a further 1.2 g of product. All three product batches were combined to give **9** (6.4 g, 46%) as a white solid: ^{1}H NMR δ (400 MHz, DMSO-d_6) 8.05 (dd, J = 8.0, 1.5 Hz, 1H), 7.68 (dd, J = 8.0, 1.5 Hz, 1H), 7.45–7.40 (m, 2H); ^{13}C NMR δ (101 MHz, DMSO-d_6) 152.2, 144.7, 143.2,

137.5, 132.7, 131.9, 130.4, 128.4, 127.0, 126.6; LCMS (ESI) RT = 1.06 min, 97% pure, *m*/*z* 372/374/376 $[M + H]^+$, and RT = 1.13 min, 3% (another isomer). Anal. Calcd for $C_{10}H_6Cl_4N_3O_2S$ = 371.8929. Found = 371.8933 $[M + H]^+$.

2,3-Dichloro-*N*-(6-chloro-3-((2-(hydroxymethyl)benzyl)oxy)-pyrazin-2-yl)benzenesulfonamide (8)

A solution of 2,3-dichloro-*N*-(3,6-dichloropyrazin-2-yl)benzenesulfonamide (2.4 g, 6.5 mmol), 1,2-phenylenedimethanol (4.5 g, 32 mmol) in NMP (40 mL) was treated with potassium *tert*-butoxide (5.47 g, 48.7 mmol) in THF (60 mL) and the mixture was stirred at room temperature for 5 h. The solution was cooled to 0 °C and 5% aqueous citric acid added (100 mL). The mixture was extracted with ethyl acetate (200 mL) and the organic solution washed with water (100 mL) and brine (100 mL) then dried over sodium sulfate and concentrated under reduced pressure. The crude material was purified by chromatography eluting with a gradient of ethyl acetate–petroleum ether (5–20%). The material recovered (1.5 g) was still impure so it was further purified by chromatography eluting with a gradient of MeOH–DCM (1–2%). The appropriate fractions were evaporated under reduced pressure and the residue was triturated with diethyl ether to give the desired material (390 mg). The filtrates from the trituration were evaporated and triturated again with petroleum ether in DCM to give a further batch of product (130 mg). The batches were combined to afford **8** (520 mg, 17%) as a solid: ^{1}H NMR (400 MHz, CD_3OD) 8.23 (dd, *J* = 8.0, 1.5 Hz, 1H), 7.78 (dd, *J* = 8.0, 1.5 Hz, 1H), 7.66 (br s, 1H), 7.49 (t, *J* = 8.0 Hz, 1H), 7.46–7.42 (m, 2H), 7.38–7.27 (m, 2H), 5.54 (s, 2H), 4.74 (s, 2H) (the NH and OH exchangeable protons were not observed); LCMS (ESI) RT = 1.22 min, 100% pure, *m*/*z* 474, 476 $[M + H]^+$. Crystal data: $C_{18}H_{14}Cl_3N_3O_4S$; *M* = 474.73; colourless needle; slow cooling from ethanol; 0.64 × 0.10 × 0.10 mm; monoclinic; space group, $P2_1/n$ (alt. $P2_1/c$, no. 14); unit cell dimensions, *a* = 9.0361(16) Å, *b* = 20.725(2) Å, *c* = 21.381(6) Å, *β* = 96.612(16)°, *V* = 3977.5(14) Å^3; *Z* = 8; d_{calc} = 1.586 Mg m^{-3}; and *μ*(Mo-Kα, *λ* = 0.71073 Å) = 0.597 mm^{-1}.

2,3-Dichloro-*N*-phenylbenzenesulfonamide (10)

Aniline (37.2 mg, 0.4 mmol) was dissolved in dichloromethane (1 mL) and treated with a solution of 2,3-dichlorobenzenesulfonyl chloride in dichloromethane (0.44 M, 1 mL, 1.1 equiv.), followed by a stock solution of pyridine in dichloromethane (10 M, 0.12 mL, 3 equiv.). The reaction mixture was stirred at room temperature for 2.5 h, and then treated with saturated aqueous sodium bicarbonate solution (2 mL). After stirring for 15 min the reaction mixture was transferred to a hydrophobic frit and the organic phase isolated. The aqueous phase was further extracted with dichloromethane (2 mL) and the combined extracts were evaporated under nitrogen in a blow-down apparatus. The product was purified by mass-directed auto-preparative HPLC (MDAP) to give **10** (84 mg, 69%): ^{1}H NMR (500 MHz, DMSO-d_6) *δ* = 10.77 (s, 1H), 8.03 (dd, *J* = 8.0, 1.5 Hz, 1H), 7.91 (dd, *J* = 8.0, 1.5 Hz, 1H), 7.53 (t, *J* = 8.0 Hz, 1H), 7.31–7.18 (m, 2H), 7.09 (d, *J* = 7.5 Hz, 2H), 7.02 (t, *J* = 7.5 Hz, 1H); ^{13}C NMR (126 MHz, DMSO-d_6) *δ* = 139.2, 137.2, 135.5, 134.7, 130.9, 129.8 (2C), 129.3, 129.1, 124.7, 119.9 (2C); LCMS (ESI) RT = 1.12 min, 100% pure, *m*/*z* = 300, 302 $[M - H]^-$. Anal. Calcd for $C_{12}H_{10}Cl_2NO_2S$ = 301.9804. Found = 301.9800 $[M + H]^+$.

2,3-Dichloro-*N*-(2-methoxyphenyl)benzenesulfonamide (11)[41]

(105 mg, 79%): ^{1}H NMR (500 MHz, DMSO-d_6) *δ* = 9.79 (s, 1H), 7.89 (dd, *J* = 8.0, 1.5 Hz, 1H), 7.76 (dd, *J* = 8.0, 1.5 Hz, 1H), 7.44 (t, *J* = 8.0 Hz, 1H), 7.23–7.10 (m, 2H), 6.95–6.78 (m, 2H), 3.44 (s, 3H); ^{13}C NMR (126 MHz, DMSO-d_6) *δ* = 153.3, 140.1, 134.1, 133.7, 129.3, 129.2, 127.8, 127.6, 127.2, 124.0, 120.3, 111.6, 54.9; LCMS (ESI) RT = 1.18 min, 98% pure, *m*/*z* 332, 334 $[M + H]^+$. Anal. Calcd for $C_{13}H_{12}Cl_2NO_3S$ = 331.9910. Found = 331.9905 $[M + H]^+$.

N-(2-Acetylphenyl)-2,3-dichlorobenzenesulfonamide (12)

2,3-Dichlorobenzenesulfonyl chloride (100 mg, 0.41 mmol) was added to a stirring solution of 2-aminoacetophenone (50 mg, 0.37 mmol) in anhydrous pyridine (2 mL) and the reaction mixture was stirred at ambient temperature for 4 h. Additional 2,3-dichlorobenzenesulfonyl chloride (75 mg, 0.30 mmol) was added and the reaction mixture was stirred for a further 18 h. The reaction mixture was evaporated under reduced pressure, and the solid was dissolved in DMSO (2 mL) and purified by MDAP. Appropriate fractions were combined and evaporated under reduced pressure to afford **12** (46 mg, 36%) as a white solid: ^{1}H NMR (500 MHz, DMSO-d_6) *δ* = 12.09 (s, 1H), 8.20 (dd, *J* = 8.0, 1.0 Hz, 1H), 8.05 (d, *J* = 8.0 Hz, 1H), 7.97 (dd, *J* = 8.0, 1.0 Hz, 1H), 7.61 (t, *J* = 8.0 Hz, 1H), 7.52 (t, *J* = 8.0 Hz, 1H), 7.36 (d, *J* = 8.0 Hz, 1H), 7.18 (t, *J* = 8.0 Hz, 1H), 2.67 (s, 3H); ^{13}C NMR (126 MHz, DMSO-d_6) *δ* = 203.8, 138.0, 138.0, 136.1, 135.5, 134.8, 133.41, 131.2, 129.2, 129.0, 123.7, 122.9, 117.4, 28.9; LCMS (ESI) RT = 1.16 min, 100% pure, *m*/*z* 344, 346 $[M + H]^+$. Anal. Calcd for $C_{14}H_{12}Cl_2NO_3S$ = 343.9910. Found = 343.9909 $[M + H]^+$.

2,3-Dichloro-*N*-(2-(1-hydroxyethyl)phenyl)benzenesulfonamide (13)

Sodium borohydride (4 mg, 0.11 mmol) was added to a stirring solution of **12** (25 mg, 0.07 mmol) in methanol (0.5 mL) and the reaction mixture was stirred at ambient temperature for 2 h. Additional sodium borohydride (4 mg, 0.11 mmol) was added and the reaction was stirred for a further 4 h. The reaction mixture was treated with 2 M HCl solution (0.1 mL), dissolved in DMSO (1 mL) and purified by MDAP. The solvent was evaporated under reduced pressure to give **13** (14 mg, 53%) as a colourless oil: ^{1}H NMR (500 MHz, DMSO-d_6) *δ* = 10.16 (br s, 1H), 8.02–7.91 (m, 2H), 7.56 (t, *J* = 8.0 Hz, 1H), 7.39 (dd, *J* = 7.5, 1.0 Hz, 1H), 7.22–7.06 (m, 2H), 6.88 (d, *J* = 8.0 Hz, 1H), 5.60 (br s, 1H), 5.05 (q, *J* = 6.3 Hz, 1H), 1.26 (d, *J* = 6.3 Hz, 3H); ^{13}C NMR (126 MHz, DMSO-d_6) *δ* = 141.2, 140.3, 135.3, 134.8, 133.4, 130.2, 129.4, 129.2, 127.8, 127.3, 126.5, 123.9, 65.8, 25.0; LCMS (ESI) RT = 1.03 min, 100% pure, *m*/*z* 344, 346 $[M + H]^+$.

N-(2-(1*H*-Pyrazol-1-yl)phenyl)-2,3-dichlorobenzenesulfonamide (14)

General procedure for the preparation of 14–20. 2,3-Dichlorobenzenesulfonyl chloride (120 mg, 0.48 mmol) was added to a stirring solution of 2-(1*H*-pyrazol-1-yl)aniline (70 mg, 0.44 mmol) in anhydrous pyridine (2 mL) and the reaction was stirred at ambient temperature for 18 h. The reaction mixture was evaporated under reduced pressure, and the solid was dissolved in DMSO (1 mL) and purified by MDAP. The solvent was evaporated under reduced pressure to **14** (118 mg, 71%) as a white solid: mp = 152–154 °C (from MeOH); ^{1}H NMR (400 MHz, DMSO-d_6) δ = 10.9 (s, 1H), 8.23 (d, J = 2.0 Hz, 1H), 7.94–7.78 (m, 3H), 7.55 (dd, J = 8.0, 2.0 Hz, 1H), 7.51–7.43 (m, 2H), 7.35–7.25 (m, 2H), 6.55 (t, J = 2.0 Hz, 1H); ^{13}C NMR (101 MHz, DMSO-d_6) δ = 141.1, 138.2, 135.1, 134.3, 131.4, 130.9, 130.0, 128.8, 128.4, 128.2, 127.9, 126.3, 123.6, 123.5, 107.5; LCMS (ESI) RT = 1.23 min, 100% pure, m/z 368, 370 $[M + H]^+$. Anal. Calcd for $C_{15}H_{12}Cl_2N_3O_2S$ = 368.0027. Found = 368.0028 $[M + H]^+$. Crystal data: $C_{15}H_{11}Cl_2N_3O_2S$; M = 368.23; colourless block; slow evaporation of methanol solution; 0.44 × 0.19 × 0.11 mm; monoclinic; space group, $P2_1/n$ (alt. $P2_1/c$, no. 14); unit cell dimensions, a = 7.5758(9) Å, b = 8.7573(9) Å, c = 23.065(2) Å, β = 91.905(8)°, V = 1529.4(3) Å^3; Z = 4; d_{calc} = 1.599 Mg m^{-3}; and μ(Mo-Kα, λ = 0.71073 Å) = 0.573 mm^{-1}.

N-(2-(1*H*-1,2,4-Triazol-1-yl)phenyl)-2,3-dichlorobenzenesulfonamide (15)

From 2-(1*H*-1,2,4-triazol-1-yl)aniline (54 mg, 0.34 mmol) and 2,3-dichlorobenzenesulfonyl chloride (91 mg, 0.37 mmol). (76 mg, 60%) as a pale yellow solid: ^{1}H NMR (400 MHz, DMSO-d_6) δ = 10.32 (br s, 1H), 8.82 (s, 1H), 8.12 (s, 1H), 7.90 (dd, J = 8.0, 1.5 Hz, 1H), 7.77 (dd, J = 8.0, 1.5 Hz, 1H), 7.55–7.51 (m, 1H), 7.49–7.38 (m, 3H), 7.34–7.28 (m, 1H); ^{13}C NMR (126 MHz, DMSO-d_6) δ = 152.5, 145.3, 139.5, 135.4, 134.8, 132.9, 130.2, 129.9, 129.6, 129.4, 129.0, 128.4, 128.2, 126.6; LCMS (ESI) RT = 0.96 min, 99% purity, m/z 369, 371 $[M + H]^+$. Anal. Calcd for $C_{14}H_{11}Cl_2N_4O_2S$ = 368.9974. Found = 368.9974 $[M + H]^+$.

N-(2-(1*H*-Tetrazol-1-yl)phenyl)-2,3-dichlorobenzenesulfonamide (16)

From 2-(1*H*-tetrazol-1-yl)aniline (84 mg, 0.34 mmol) and 2,3-dichlorobenzenesulfonyl chloride (91 mg, 0.37 mmol). (56 mg, 47%) as a white solid; mp = 188–190 °C (from MeOH); ^{1}H NMR (400 MHz, DMSO-d_6) δ = 10.56 (br s, 1H), 9.60 (s, 1H), 7.93 (dd, J = 8.0, 1.0 Hz, 1H), 7.74 (dd, J = 8.0, 1.0 Hz, 1H), 7.64–7.53 (m, 2H), 7.52–7.42 (m, 2H), 7.34–7.20 (m, 1H); ^{13}C NMR (101 MHz, DMSO-d_6) δ = 144.6, 139.2, 134.8, 134.4, 131.4, 130.4, 130.2, 129.1, 128.9, 128.6, 128.5, 128.2, 127.5; LCMS (ESI) RT = 0.92 min, 95% purity, m/z 370, 372 $[M + H]^+$. Anal. Calcd for $C_{13}H_{10}Cl_2N_5O_2S$ = 369.9932. Found = 369.9930 $[M + H]^+$. Crystal data: $C_{13}H_9Cl_2N_5O_2S$; M = 370.21; colourless rod; slow evaporation of methanol solution; 0.39 × 0.10 × 0.06 mm; triclinic; space group, $P\bar{1}$ (no. 2); unit cell dimensions, a = 7.4390(9) Å, b = 8.4770(12) Å, c = 13.0579(15) Å, α = 88.763(11)°, β = 84.177(10)°, γ = 64.880(13)°, V = 741.50(16) Å^3; Z = 2; d_{calc} = 1.658 Mg m^{-3}; and μ(Mo-Kα, λ = 0.71073 Å) = 0.595 mm^{-1}.

2,3-Dichloro-*N*-(2-(oxazol-5-yl)phenyl)benzenesulfonamide (17)

From 2-(oxazol-5-yl)aniline (54 mg, 0.34 mmol) and 2,3-dichlorobenzenesulfonyl chloride (91 mg, 0.37 mmol). (77 mg, 61%) as a pale yellow solid; ^{1}H NMR (400 MHz, DMSO-d_6) δ = 10.29 (s, 1H), 8.39 (s, 1H), 7.92 (dd, J = 8.0, 1.5 Hz, 1H), 7.78 (dd, J = 8.0, 1.5 Hz, 1H), 7.68 (dd, J = 7.7, 1.5 Hz, 1H), 7.60 (s, 1H), 7.49 (t, J = 8.0 Hz, 1H), 7.40 (t, J = 7.7 Hz, 1H), 7.30 (td, J = 7.7, 1.5 Hz, 1H), 6.91 (dd, J = 7.7, 1.5 Hz, 1H); ^{13}C NMR (126 MHz, DMSO-d_6 + $NaHCO_3$) δ = 150.5, 149.7, 147.5, 147.1, 133.6, 131.5, 129.3, 128.9, 128.1, 127.7, 125.3, 125.0, 119.6, 119.4, 116.7; LCMS (ESI) RT = 1.00 min, 100% pure, m/z 369, 371 $[M + H]^+$. Anal. Calcd for $C_{15}H_{11}Cl_2N_2O_3S$ = 368.9862. Found = 368.9860 $[M + H]^+$.

2,3-Dichloro-*N*-(2-(5-methyl-1,3,4-oxadiazol-2-yl)phenyl)-benzenesulfonamide (18)

From 2-(5-methyl-1,3,4-oxadiazol-2-yl)aniline (59 mg, 0.34 mmol) and 2,3-dichlorobenzenesulfonyl chloride (91 mg, 0.37 mmol). (46 mg, 35%) as a white solid: ^{1}H NMR (400 MHz, DMSO-d_6) δ = 11.21 (s, 1H), 8.19 (dd, J = 8.0, 1.5 Hz, 1H), 7.97 (dd, J = 8.0, 1.5 Hz, 1H), 7.88 (d, J = 7.5 Hz, 1H), 7.61 (t, J = 8.0 Hz, 1H), 7.56–7.41 (m, 2H), 7.28 (t, J = 7.5 Hz, 1H), 2.60 (s, 3H); ^{13}C NMR (126 MHz, DMSO-d_6) δ = 164.1, 163.3, 138.3, 136.2, 135.6, 135.0, 133.4, 131.2, 129.4, 129.2, 129.1, 124.9, 118.7, 112.4, 11.1; LCMS (ESI) RT = 1.17 min, 100% pure, m/z 384, 386 $[M + H]^+$. Anal. Calcd for $C_{15}H_{12}Cl_2N_3O_3S$ = 383.9971. Found = 383.9967 $[M + H]^+$.

2,3-Dichloro-*N*-[2-(1*H*-pyrazol-1-yl)-3-pyridinyl]-benzenesulfonamide (19)

From 2-(1*H*-pyrazol-1-yl)-3-pyridinamine (59 mg, 0.37 mmol) and 2,3-dichlorobenzenesulfonyl chloride (100 mg, 0.41 mmol). (83 mg, 60%) as a white solid: mp = 135–138 °C; ^{1}H NMR (400 MHz, DMSO-d_6) δ = 12.08 (s, 1H), 8.62 (d, J = 2.0 Hz, 1H), 8.21 (d, J = 4.0 Hz, 1H), 8.10 (dd, J = 8.0, 1.0 Hz, 1H), 8.04 (s, 1H), 8.00–7.86 (m, 2H), 7.56 (t, J = 8.0 Hz, 1H), 7.34 (dd, J = 8.0, 4.0 Hz, 1H), 6.67 (d, J = 2.0 Hz, 1H); ^{13}C NMR (101 MHz, DMSO-d_6) δ = 143.3, 141.7, 138.6, 137.4, 135.6, 134.5, 130.5, 129.6, 128.9, 128.8, 128.7, 123.6, 122.8, 107.7; LCMS (ESI) RT = 0.80 min, 98% pure, m/z 369, 371 $[M + H]^+$. Anal. Calcd for $C_{14}H_{11}Cl_2N_4O_2S$ = 368.9980. Found = 368.9971 $[M + H]^+$.

N-(4-(1*H*-Pyrazol-1-yl)pyridin-3-yl)-2,3-dichlorobenzenesulfonamide (20)

From 4-(1*H*-pyrazol-1-yl)pyridin-3-amine (50 mg, 0.31 mmol) and 2,3-dichlorobenzenesulfonyl chloride (84 mg, 0.34 mmol). (57 mg, 47%) as a pale brown solid: mp = 188–191 °C; ^{1}H NMR (500 MHz, DMSO-d_6 + $NaHCO_3$) δ = 9.43 (d, J = 2.5 Hz, 1H), 8.34 (s, 1H), 8.03 (dd, J = 8.0, 1.5 Hz, 1H), 7.79 (d, J = 8.0 Hz, 1H), 7.71–7.57 (m, 3H), 7.41 (t, J = 8.0 Hz, 1H), 6.44 (t, J = 2.1 Hz, 1H); the exchangeable NH proton was not observed;

^{13}C NMR (126 MHz, DMSO-d_6 + $NaHCO_3$) δ = 146.6, 143.2, 139.8, 138.1, 135.9, 135.7, 133.5, 132.9, 131.7, 129.0, 128.8, 127.7, 115.4, 106.0; LCMS (ESI) RT = 0.98 min, 95% pure, *m*/*z* 369, 371 $[M + H]^+$. Anal. Calcd for $C_{14}H_{11}Cl_2N_4O_2S$ = 368.9974. Found = 368.9974 $[M + H]^+$.

3-(1*H*-Pyrazol-1-yl)pyridin-2-amine (25)[33]

A mixture of 3-bromopyridin-2-amine (**24**) (500 mg, 2.89 mmol), potassium carbonate (839 mg, 6.07 mmol), *N*,*N*′-dimethylethylenediamine (0.092 mL, 0.87 mmol), pyrazole (236 mg, 3.47 mmol) and CuI (83 mg, 0.43 mmol) in *p*-xylene (8 mL) was heated under nitrogen at 142 °C for 72 h. The mixture was partitioned between ethyl acetate (100 mL) and water (50 mL). The organic layer was separated, washed with brine (50 mL), dried ($MgSO_4$) and evaporated under reduced pressure. The sample was pre-absorbed on Florisil and purified by chromatography on a silica cartridge (100 g), using a gradient of 0–50% ethyl acetate–cyclohexane over 40 min. The appropriate fractions were combined and the solvent was evaporated under reduced pressure to give **25** (230 mg, 50%) as a beige coloured solid: ^{1}H NMR (400 MHz, $CDCl_3$) δ = 8.07 (d, *J* = 5.0 Hz, 1H), 7.85–7.65 (m, 2H), 7.44 (dd, *J* = 8.0, 1.5 Hz, 1H), 6.71 (dd, *J* = 8.0, 5.0 Hz, 1H), 6.47 (t, *J* = 2.0 Hz, 1 H), 5.75 (br s, 2H); LCMS (ESI) RT = 0.61 min, 100% pure, *m*/*z* 161 $[M + H]^+$.

N-(3-(1*H*-Pyrazol-1-yl)pyridin-2-yl)-2,3-dichlorobenzenesulfonamide (23)

From **25** (15 mg, 0.09 mmol) and 2,3-dichlorobenzenesulfonyl chloride (25 mg, 0.10 mmol) (14 mg, 41%) as a white solid: mp = 199–202 °C; ^{1}H NMR (500 MHz, DMSO-d_6 + $NaHCO_3$) δ = 9.10 (d, *J* = 2.0 Hz, 1H), 8.03 (dd, *J* = 8.0, 1.5 Hz, 1H), 7.77 (dd, *J* = 8.0, 1.5 Hz, 1H), 7.66–7.52 (m, 3H), 7.36 (t, *J* = 8.0 Hz, 1H), 6.52 (dd, *J* = 8.0, 5.0 Hz, 1H), 6.40 (t, *J* = 2.0 Hz, 1H); the exchangeable NH proton was not observed; ^{13}C NMR (126 MHz, DMSO-d_6 + $NaHCO_3$) δ = 152.2, 147.7, 144.8, 139.3, 132.6, 131.9, 131.0, 130.1, 128.8, 128.5, 127.1, 126.0, 112.0, 105.3; LCMS (ESI) RT = 1.02 min, 100% pure, *m*/*z* 369, 371 $[M + H]^+$. Anal. Calcd for $C_{14}H_{11}Cl_2N_4O_2S$ = 368.9974. Found = 368.9974 $[M + H]^+$.

4-Nitro-3-(1*H*-pyrazol-1-yl)pyridine (28)

Sodium hydride (113 mg of a 60% w/w dispersion in mineral oil, 2.82 mmol) was added to a stirred solution of 1*H*-pyrazole (287 mg, 4.22 mmol) in NMP (5 mL) at 0 °C. The mixture was stirred for 5 min, then 3-fluoro-4-nitropyridine (**27**) (200 mg, 1.41 mmol) was added and the reaction was heated to 100 °C for 18 h. After cooling, ethyl acetate (50 mL) and water (50 mL) were poured into the mixture. The organic layer was separated, washed with water (50 mL), brine (30 mL), dried ($MgSO_4$), and evaporated under reduced pressure. The sample was purified by chromatography on a silica cartridge (70 g) using a gradient of 25–100% ethyl acetate–cyclohexane over 40 min. The appropriate fractions were combined and evaporated under reduced pressure to give **28** (173 mg, 64%) as a white solid: ^{1}H NMR (400 MHz, DMSO-d_6) δ = 9.10 (d, *J* = 2.0 Hz, 1H), 8.57–8.41 (m, 3H), 7.86 (d, *J* = 2.0 Hz, 1H), 6.64 (t, *J* = 2.0 Hz, 1H); ^{13}C NMR (126 MHz, DMSO-d_6) δ = 153.8, 143.9, 140.3, 138. 6, 129.9, 129.0, 120.3, 110.3; LCMS (ESI) RT = 0.70 min, 98% pure, *m*/*z* 191 $[M + H]^+$. Anal. Calcd for $C_8H_7N_4O_2$ = 191.0564. Found = 191.0560 $[M + H]^+$.

3-(1*H*-Pyrazol-1-yl)pyridin-4-amine (29)

Tin(II) chloride (449 mg, 2.37 mmol) was added to a solution of **28** (90 mg, 0.47 mmol) in MeOH (1.5 mL). Conc. HCl (0.2 mL of a 12 M solution, 2.4 mmol) was added and the reaction mixture was allowed to stir at ambient temperature for 48 h. The reaction mixture was neutralised by the addition of solid sodium carbonate. The solution was diluted with ethyl acetate (100 mL), washed with sodium hydroxide (20 mL of a 1 M aqueous solution), followed by sodium bicarbonate (40 mL of a saturated aqueous solution), dried ($MgSO_4$), and concentrated under reduced pressure to give **29** (55 mg, 68%) as a white solid: ^{1}H NMR (400 MHz, DMSO-d_6) δ = 8.32 (d, *J* = 3.0 Hz, 1H), 8.23 (d, *J* = 3.0 Hz, 1H), 7.77 (dd, *J* = 8.0, 2.0 Hz, 1H), 7.65 (d, *J* = 2.0 Hz, 1H), 6.54 (d, *J* = 8.0 Hz, 1H), 6.46 (t, *J* = 2.0 Hz, 1H), 6.06 (br s, 2H); LCMS (ESI) RT = 0.33 min, 93% pure, *m*/*z* 161 $[M + H]^+$.

N-(3-(1*H*-Pyrazol-1-yl)pyridin-4-yl)-2,3-dichlorobenzenesulfonamide (26)

From **29** (35 mg, 0.22 mmol) and 2,3-dichlorobenzenesulfonyl chloride (70 mg, 0.28 mmol) (42 mg, 51%) as a pale brown solid: mp = 246–250 °C; ^{1}H NMR (400 MHz, DMSO-d_6) δ = 11.90 (br s, 1H), 8.52 (br s, 1H), 8.41 (d, *J* = 2.5 Hz, 1H), 8.16 (m, 2H), 7.91 (d, *J* = 7.5 Hz, 1H), 7.73 (d, *J* = 1.5 Hz, 1H), 7.59 (t, *J* = 8.0 Hz, 1H), 7.19 (br s, 1H), 6.52 (t, *J* = 2.5 Hz, 1H); ^{13}C NMR (126 MHz, DMSO-d_6 + $NaHCO_3$) δ = 160.2, 147.5, 140.5, 138.8, 133.2, 131.5, 129.7, 129.2, 128.4, 128.1, 127.8, 127.5, 114.8, 107.4; LCMS (ESI) RT = 0.94 min, 98% pure, *m*/*z* 369, 371 $[M + H]^+$. Anal. Calcd for $C_{14}H_{11}C_{l2}N_4O_2S$ = 368.9974. Found = 368.9974 $[M + H]^+$.

N-(3-Bromopyrazin-2-yl)-2,3-dichlorobenzenesulfonamide (32)

Sodium hydride (575 mg of a 60% w/w dispersion in mineral oil, 14.4 mmol) was added to a stirred solution of 3-bromopyrazin-2-amine (**31**) (500 mg, 2.87 mmol) in anhydrous DME (6 mL) at 0 °C. The mixture was stirred for 30 min and then 2,3-dichlorobenzenesulfonyl chloride (776 mg, 3.16 mmol) was added. The reaction was allowed to warm to ambient temperature and stirred for 18 h. The reaction mixture was quenched by the addition of HCl (20 ml of a 2 M aqueous solution) and the product was extracted with ethyl acetate (3 × 50 mL). The organic extracts were combined, dried ($MgSO_4$), and evaporated under reduced pressure to give the crude product. The residue was adsorbed onto Florisil, and purified by chromatography on a silica cartridge (50 g) eluting with a gradient of 0–100% ethyl acetate–cyclohexane over 40 min. The appropriate fractions were combined and evaporated under reduced pressure to give **32** (800 mg, 73%) as a beige coloured solid: ^{1}H NMR (600 MHz, DMSO-d_6) δ = 8.15 (br s, 1H), 8.12 (br s, 1H), 8.06 (dd, *J* = 8.1, 1.5 Hz, 1H), 7.93 (dd, *J* = 8.1, 1.5 Hz, 1H), 7.58 (t, *J* = 8.1 Hz, 1H); the exchangeable NH proton was not

observed; ^{13}C NMR (151 MHz, CD_3OD + DCl) δ = 146.6, 141.4, 141.1, 139.2, 138.5, 136.1, 136.0, 132.3, 131.0, 128.9; LCMS (ESI) RT = 0.98 min, 91% pure, *m*/*z* 382, 384, 386 $[M + H]^+$. Anal. Calcd for $C_{10}H_7BrCl_2N_3O_2S$ = 381.8814. Found = 381.8819, $[M + H]^+$.

N-(3-(1*H*-Pyrazol-1-yl)pyrazin-2-yl)-2,3-dichlorobenzene-sulfonamide (30)

Sodium hydride (60% oil dispersion, 52 mg, 1.3 mmol) was added to a stirred solution of 1*H*-pyrazole (107 mg, 1.57 mmol) in NMP (1.0 mL) at 0 °C. The mixture was stirred for 5 min, then **32** (100 mg, 0.261 mmol) was added and the reaction was heated to 100 °C for 18 h. After cooling, the mixture was poured into water (20 mL), acidified to pH 5 with 2 M aqueous HCl solution. Ethyl acetate (20 mL) was poured into the mixture, and the organic layer was separated, washed with water (20 mL), brine (20 mL), dried through a frit, and evaporated under reduced pressure. The crude product was triturated with MeOH to give **30** (68 mg, 71%) as a white solid: mp = 217–220 °C; ^{1}H NMR (400 MHz, DMSO-d_6) δ = 12.32 (br s, 1H), 8.77 (d, *J* = 2.5 Hz, 1H), 8.28 (dd, *J* = 8.0, 1.5 Hz, 1H), 8.19 (d, *J* = 2.5 Hz, 1H), 8.15 (d, *J* = 1.5 Hz, 1H), 8.12 (d, *J* = 2.5 Hz, 1H), 7.98 (dd, *J* = 8.0, 1.5 Hz, 1H), 7.65 (t, *J* = 8.0 Hz, 1H), 6.80–6.75 (m, 1H); ^{13}C NMR (126 MHz, DMSO-d_6) δ = 142.9, 140.0, 139.1, 138.0, 136.8, 135.9, 134.5, 134.2, 131.9, 130.1, 129.2, 109.3 1C missing; LCMS (ESI) RT = 1.18 min, 100% pure, *m*/*z* 370, 372 $[M + H]^+$ = 370, 372. Anal. Calcd for $C_{13}H_{10}Cl_2N_5O_2S$ = 369.9927. Found = 369.9931 $[M + H]^+$.

N-(3-(1*H*-Pyrazol-1-yl)pyridin-2-yl)-5-chlorothiophene-2-sulfonamide (33)

From **25** (40 mg, 0.25 mmol) and 5-chlorothiophene-2-sulfonyl chloride (60 mg, 0.28 mmol) (26 mg, 57%) as a white solid: ^{1}H NMR (500 MHz, DMSO-d_6 + $NaHCO_3$) δ = 8.91 (d, *J* = 2.0 Hz, 1H), 7.98 (dd, *J* = 5.0, 2.0 Hz, 1H), 7.82 (dd, *J* = 8.0, 2.0 Hz, 1H), 7.61 (d, *J* = 2.0 Hz, 1H), 7.30 (d, *J* = 4.0 Hz, 1H), 6.94 (d, *J* = 4.0 Hz, 1H), 6.65 (dd, *J* = 8.0, 5.0 Hz, 1H), 6.39 (t, *J* = 2.0 Hz, 1H), the exchangeable NH proton was not observed; ^{13}C NMR (126 MHz, DMSO-d_6 + $NaHCO_3$) δ = 152.4, 148.8, 144.8, 139.6, 132.1, 130.3, 129.4, 127.6, 126.3, 125.7, 112.6, 105.6; LCMS (ESI) RT = 1.00 min, 95% pure, *m*/*z* 341, 343 $[M + H]^+$. Anal. Calcd for $C_{12}H_{10}ClN_4O_2S_2$ = 340.9928. Found = 340.9928 $[M + H]^+$.

Acknowledgements

We thank Mike Woodrow and Steve Sollis for the synthesis of **7**, Viqui Vinader for crystallising **8**, Sean Lynn and Steve Richards for some NMR spectra, Bill J. Leavens for collecting the HRMS data, the Screening and Compound Profiling Department at GlaxoSmithKline for generating the human CCR4 GTPγS data, Tao Pun and Sally-Anne Rumley for the whole blood assay, and Professor W. Clegg, Dr N. R. Brooks, Dr L. Russo and Dr R. W. Harrington for the GSK funded crystal structures of **7**, **8**, **14** and **16**.

References

1 P. J. Koelink, S. A. Overbeek, S. Braber, P. de Kruijf, G. Folkerts, M. J. Smit and A. D. Kraneveld, *Pharmacol. Ther.*, 2012, **133**, 1.
2 J. Pease and R. Horuk, *J. Med. Chem.*, 2012, **55**, 9363.
3 J. M. Rolland, J. Douglass and R. E. O'Hehir, *Expert Opin. Invest. Drugs*, 2000, **9**, 515.
4 A. E. I. Proudfoot, *Nat. Rev. Immunol.*, 2002, **2**, 106.
5 P. Panina-Bordignon, A. Papi, M. Mariani, P. D. Lucia, G. Casoni, C. Bellettato, C. Buonsanti, D. Miotto, C. Mapp, A. Villa, G. Arrigoni, L. M. Fabri and F. Sinigaglia, *J. Clin. Invest.*, 2001, **107**, 1357.
6 P. Vijayanand, K. Durkin, G. Hartmann, J. Morjaria, G. Seumois, K. J. Staples, D. Hall, C. Bessant, M. Bartholomew, P. H. Howarth, P. S. Friedmann and R. Djukanović, *J. Immunol.*, 2010, **184**, 4568.
7 S. Rahman, M. Collins, C. M. M. Williams and H.-L. Ma, *Inflammation Allergy: Drug Targets*, 2011, **10**, 486.
8 D. Hartl, K. F. Buckland and C. M. Hogaboam, *Inflammation Allergy: Drug Targets*, 2006, **5**, 219.
9 T. Ishida and R. Ueda, *Int. J. Hematol.*, 2011, **94**, 443.
10 R. Guabiraba, R. E. Marques, A.-G. Besnard, C. T. Fagundes, D. G. Souza, B. Ryffel and M. M. Teixeira, *PLoS One*, 2010, **5**(12), e15680.
11 G. Banfield, H. Watanabe, G. Scadding, M. R. Jacobson, S. J. Till, D. A. Hall, D. S. Robinson, C. M. Lloyd, K. T. Nouri-Aria and S. R. Durham, *Allergy*, 2010, **65**, 1126.
12 A. V. Purandare and J. E. Somerville, *Curr. Top. Med. Chem.*, 2006, **6**, 1335.
13 X. Wang, F. Xu, Q. Xu, H. Mahmud, J. Houze, L. Zhu, M. Akerman, G. Tonn, L. Tang, B. E. McMaster, D. J. Dairaghi, T. J. Schall, T. L. Collins and J. C. Medina, *Bioorg. Med. Chem. Lett.*, 2006, **16**, 2800.
14 A. V. Purandare, H. Wan, J. E. Somerville, C. Burke, W. Vaccaro, X. Yang, K. W. McIntyre and M. A. Poss, *Bioorg. Med. Chem. Lett.*, 2007, **17**, 679.
15 C. F. Kuhn, M. Bazin, L. Philippe, J. Zhang, L. Tylaska, J. Miret and P. H. Bauer, *Chem. Biol. Drug Des.*, 2007, **70**, 268.
16 D. F. Burdi, S. Chi, K. Mattia, C. Harrington, Z. Shi, S. Chen, S. Jacutin-Porte, R. Bennett, K. Carson, W. Yin, V. Kansra, J.-A. Gonzalo, A. Coyle, B. Jaffee, T. Ocain, M. Hodge, G. LaRosa and G. Harriman, *Bioorg. Med. Chem. Lett.*, 2007, **17**, 3141.
17 K. Yokoyama, N. Ishikawa, S. Igarashi, N. Kawano, N. Masuda, K. Hattori, T. Miyazaki, S.-I. Ogino, M. Orita, Y. Matsumoto, M. Takeuchi and M. Ohta, *Bioorg. Med. Chem.*, 2008, **16**, 7968.
18 Y. Nakagami, K. Kawashima, K. Yonekubo, M. Etori, T. Jojima, S. Miyazaki, R. Sawamura, K. Hirahara, F. Nara and M. Yamashita, *Eur. J. Pharmacol.*, 2009, **624**, 38.
19 K. Yokoyama, N. Ishikawa, S. Igarashi, N. Kawano, N. Masuda, W. Hamaguchi, S. Yamasaki, Y. Koganemaru, K. Hattori, T. Miyazaki, T. Miyazaki, S.-I. Ogino, Y. Matsumoto, M. Takeuchi and M. Ohta, *Bioorg. Med. Chem.*, 2009, **17**, 64.

20 F. Zhao, J.-H. Xiao, Y. Wang and S. Li, *Chin. Chem. Lett.*, 2009, **20**, 296.
21 Y. Nakagami, Y. Kawase, K. Yonekubo, E. Nosaka, M. Etori, S. Takahashi, N. Takagi, T. Fukuda, T. Kuribayashi, F. Nara and M. Yamashita, *Biol. Pharm. Bull.*, 2010, **33**, 1067.
22 Y. Nakagami, K. Kawashima, M. Etori, K. Yonekubo, C. Suzuki, T. Jojima, T. Kuribayashi, F. Nara and M. Yamashita, *Basic Clin. Pharmacol. Toxicol.*, 2010, **107**, 793.
23 A. Baxter, T. Johnson, N. Kindon, B. Roberts and M. Stocks, WO2003059893A1 (24 Jul 2003).
24 H. Habashita, M. Kokubo, S. Shibayama, H. Tada and K. Sagawa, WO2004007472A1 (22 Jan 2004).
25 P. A. Procopiou, A. J. Ford, R. H. Graves, D. A. Hall, S. T. Hodgson, Y. M. L. Lacroix, D. Needham and R. J. Slack, *Bioorg. Med. Chem. Lett.*, 2012, **22**, 2730.
26 P. A. Procopiou, J. W. Barrett, N. P. Barton, M. Begg, D. Clapham, R. C. B. Copley, A. J. Ford, R. H. Graves, D. A. Hall, A. P. Hancock, A. P. Hill, H. Hobbs, S. T. Hodgson, C. Jumeaux, Y. M. L. Lacroix, A. H. Miah, K. M. L. Morriss, D. Needham, E. B. Sheriff, R. J. Slack, C. E. Smith, S. L. Sollis and H. Staton, *J. Med. Chem.*, 2013, **56**, 1946.
27 R. J. Slack, L. J. Russell, N. P. Barton, C. Weston, G. Nalesso, S.-A. Thompson, M. Allen, Y.-H. Chen, A. Barnes, S. T. Hodgson and D. A. Hall, Antagonism of human CC-chemokine receptor 4 can be achieved through three distinct binding sites on the receptor, *Pharmacol. Res. Perspect.*, 2013, **1**, e00019.
28 A. Cahn, S. Hodgson, R. Wilson, J. Robertson, J. Watson, M. Beerahee, S. C. Hughes, G. Young, R. Graves, D. Hall, S. Van Marle and R. Solari, *BMC Pharmacol. Toxicol.*, 2013, **14**, 14.
29 V. H. Thomas, S. Bhattachar, L. Hitchingham, P. Zocharski, M. Naath, N. Surendran, C. L. Stoner and A. El-Kattan, *Expert Opin. Drug Metab. Toxicol.*, 2006, **2**, 591.
30 B. Kuhn, P. Mohr and M. Stahl, *J. Med. Chem.*, 2010, **53**, 2601.
31 R. J. Slack and D. A. Hall, *Br. J. Pharmacol.*, 2012, **166**, 1774.
32 E. M. Bomhard and B. A. Herbold, *Crit. Rev. Toxicol.*, 2005, **35**, 783.
33 J. D. Culshaw, J. M. Eden, S. J. Ford, B. Hayter, D. R. Perkins and K. G. Pike, *Synlett*, 2012, 1816.
34 Wavefunction, Irvine, CA, 2008.
35 A. D. Becke, *J. Chem. Phys.*, 1993, **98**, 5648.
36 C. T. Lee, W. T. Yang and R. G. Parr, *Physical Rev. B: Condens. Matter*, 1988, **37**, 785.
37 A. C. Chamberlin, C. J. Cramer and D. G. Truhlar, *J. Phys. Chem. B*, 2008, **112**, 8651.
38 C. J. Cramer and D. G. Truhlar, *Acc. Chem. Res.*, 2008, **41**, 760.
39 H.-J. Liu, S.-F. Hung, C.-L. Chen and M.-H. Lin, *Tetrahedron*, 2013, **69**, 3907.
40 G. Palamidessi, L. Bernardi and A. Leone, *Farmaco, Ed. Sci.*, 1966, **21**, 805.
41 A. Marei, M. M. A. El-Sukkary, F. I. El-Dib and O. H. El-Sayed, *Hung. J. Ind. Chem.*, 1981, **9**, 417.